Scilight

Plant Ecophysiology
www.sciltp.com/journals/PlantEcophys

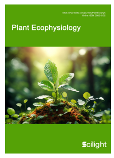

Article

Evaluation of Grafting Method and Scion—Rootstock Alignment Effects on Anatomical Development and Hydraulic Properties of Grapevine (*Vitis vinifera* L.) Graft Unions

Ana Villa-Llop [1,2,3,*], Sara Crespo-Martínez [2,3], Maite Loidi [3], Ana Pina [4,5], Patricia Irisarri [4,5] and Luis Gonzaga Santesteban [2,3]

[1] Vitis Navarra Nursery, 31251 Larraga, Spain
[2] Institute for Multidisciplinary Research in Applied Biology (IMAB-UPNA), Public University of Navarre, Campus Arrosadia, 31006 Pamplona, Spain
[3] Department of Agronomy, Biotechnology and Food Science, Public University of Navarre, 31006 Pamplona, Spain
[4] Centro de Investigación y Tecnología Agroalimentaria de Aragón (CITA), Departamento de Ciencia Vegetal, Avenida Montañana 930, 50059 Zaragoza, Spain
[5] Instituto Agroalimentario de Aragón-IA2, CITA-Universidad de Zaragoza, 50013 Zaragoza, Spain
* Correspondence: ana.villa@unavarra.es

How To Cite: Villa-Llop A, Crespo-Martínez SC, Loidi M, Pina A, Irisarri P, & Santesteban LG. Evaluation of Grafting Method and Scion—Rootstock Alignment Effects on Anatomical Development and Hydraulic Properties of Grapevine (*Vitis vinifera* L.) Graft Unions. *Plant Ecophysiology* **2026**, *2*(1), 2. https://doi.org/10.53941/plantecophys.2026.100002

Publication History
Received: 20 October 2025
Revised: 5 March 2026
Accepted: 7 March 2026
Published: 13 March 2026

Abstract: Evaluating graft quality in grapevine grafted plants is challenging because structural differences at the graft union are mostly internal. Conventional nursery assessments rely on external inspection, which provides limited information on vascular reconnection. This study applied two complementary approaches to characterise graft union quality: histological observations of callus and vascular development, and hydraulic conductance measurements. Trials were conducted in 2020 and 2021 with Tempranillo grafted onto 110 Richter. Five bench grafting methods were tested: omega with completely aligned cambium (OM-CA), omega with partially aligned cambium (OM-PA), V-shape (V), full cleft (FC), and hand-made whip and tongue (WTh). Histological analysis based on phenotyping of graft union vascular development were done at two time points, after the callusing phase and after field rooting, and hydraulic conductance was measured in one-year-old potted plants using a gravimetric flow–pressure method. Omega grafts, despite shorter contact surfaces, generally produced higher callus and a greater proportion of plants with complete vascular connection. OM-CA reached the most advanced vascular developmental categories, whereas V and WTh remained in intermediate stages and FC showed variable results. Hydraulic conductance did not differ among methods, although OM-CA displayed the highest and most uniform values. These results indicated that grafting efficiency depended more on cambial alignment and tissue differentiation than on the length of cambium surface. Combining scalable histological and hydraulic measurements offered a practical framework to assess graft quality in nursery trials and complemented advanced imaging approaches.

Academic Editor
Sigfredo Fuentes

Keywords: callus formation; cambium; conductance; nursery propagation

1. Introduction

Grafting is a horticultural practice defined as the natural or deliberate fusion of plant parts to establish vascular continuity between them (Pina & Errea, 2005), resulting in a genetically composite organism that functions as a single plant (Mudge et al., 2009). The origin of grafting is unknown, but it is probable that early grafters were inspired by natural grafting, a phenomenon in which trunks, arms and roots of woody species spontaneously fuse within or between plants (Mudge et al., 2009). The conditions that allow natural graft formation, such as compatibility, cambial alignment and contact, adequate pressure, and protection from desiccation, are still required for successful deliberate grafting (Mudge et al., 2009).

The process of graft union formation is complex and the mechanisms responsible for such integration remain poorly understood. It involves the differentiation of cambial cells, and the subsequent formation of vascular tissue, beginning with phloem and followed by xylem (Melnyk, 2017; Melnyk et al., 2018, Melnyk & Meyerowitz, 2015). In addition, recent studies have shown that graft union formation is associated with molecular and transcriptional reprogramming at the graft interface, coordinating wound responses, cell proliferation, and vascular regeneration (Melnyk et al., 2018; Loupit et al., 2025). This tissue differentiation and regeneration in both rootstock and scion, allows the vascular continuity between the partners (Pina et al., 2017).

In viticulture, grafting became essential after the accidental introduction of phylloxera (*Daktulosphaira vitifoliae*) in Europe in the second half of the 19th century. Susceptible *Vitis vinifera* L. scions were grafted onto phylloxera-resistant rootstocks derived from *Vitis* spp., which allowed the reconstruction of European vineyards (Ollat et al., 2016). Since then, grafting methods have evolved from traditional field techniques to mechanized dormant bench grafting, and from hand-made methods such as the full cleft (FC) and whip-and-tongue (WTh) to the widespread adoption of the omega graft (OM), particularly after its mechanization in the 1980s (Camboué et al., 2025). However, there is an increasing concern regarding the implications of grafting practices on vineyard performance. These concerns include the general quality of the vascular connections in grafted plants (Bahar et al., 2010; Korkutal, Bahar, & Ozdemir, 2018; Marín et al., 2022), and the specific influence of the graft method (Battiston et al., 2022; Camboué et al., 2025; Janoueix et al., 2024; Mary et al., 2017; Villa-Llop et al., 2025). Vine decline and premature mortality in young vineyards have been associated with weaknesses at the graft union (Stamp, 2001), highlighting the need to understand how grafting method influences both short-term nursery success and long-term vineyard performance (Marín et al., 2022; Villa-Llop et al., 2025).

The evaluation of grafting quality is challenging, as differences at the graft union are often internal and not readily visible from external inspection. In commercial nurseries, assessment is commonly limited to the "thumb test", which only evaluates mechanical stability (Carrere et al., 2022). Furthermore, this method is non-quantifiable due to the lack of mechanisation and exhibits low reproducibility. In the last decade, several studies have investigated the anatomical structure of the graft union using two- and three-dimensional techniques (Bahar et al., 2010; Battiston et al., 2022; Camboué et al., 2025; Spilmont et al., 2021; Tedesco et al., 2023). These approaches have provided high quality information on the structural organization of the grafting union, but techniques such as tomography and three-dimensional micro-computed tomography (micro-CT) require specialised infrastructures and limit the analysis to a reduced number of plants.

Therefore, there is a need for using characterization approaches that can provide information on graft union development in larger numbers of plants under nursery conditions. Within this context, the present study aimed to evaluate graft union development in one-year-old grafted plants produced by different bench grafting methods, using scalable approaches based on histological observations and hydraulic conductance measurements.

2. Material and Methods

2.1. Plant material and experimental design

Scion and rootstock material were collected during winter from certified mother fields managed by Vitis Navarra S.A.T. (Larraga, Navarra, Spain; 42°27′45″ N, 1°48′13″ W; 325 m a.s.l.). Tempranillo (*V. vinifera*, clone VN69) was used as scion, grafted onto 110 Richter rootstock (*V. berlandieri* × *V. rupestris*, clone 237). Tempranillo is one of the most widely cultivated grapevine cultivars in Spain, while 110R accounts for approximately 60% of the grafted plant production in the country, and show good graft compatibility (Marín et al., 2019).

The experimental layout consisted of two consecutive trials conducted in 2020 and 2021 at the Vitis Navarra S.A.T. nursery, using different bench grafting methods (Figure 1). In 2020, five grafting methods were evaluated: omega with completely aligned cambium (OM-CA), omega with partially aligned cambium (OM-PA), V-shape (V), full cleft (FC), and hand-made whip and tongue (WTh). In 2021, FC was excluded due to poor shoot and root development and low structural integrity at the graft union. Further details on the grafting procedure are available in Villa-Llop et al. (2025).

Each method followed specific operational procedures, 150 plants were grafted per grafting modality per year. In short, OM grafting was performed using the Omega Star® foot-drive machine (Wahler OMEGA GmbH & Co. KG, Weinstadt-Schnait, Germany), producing complementary convex (scion) and concave (rootstock) omega cuts. For OM-CA, scion and rootstock cuttings with closely matched diameters were used to maximize cambial contact. For OM-PA, mismatched diameters were deliberately selected, aligning the cambium on one side only to simulate partial contact, as described by Marín et al. (2022). V-shape grafting was semi-mechanized using the Graftech® machine (Raggett Industries Ltd., Gisborne, New Zealand). The rootstock cutting was cut into a V, and the scion into an inverted V. Unions were manually attached using natural rubber grafting tape. FC grafts involved a mechanically cut inverted V in the scion and a longitudinal manual split in the rootstock, followed by manual attachment and taping. WTh was performed entirely manually by a trained grafter using a grafting knife, producing a Z-shaped interface, without tape.

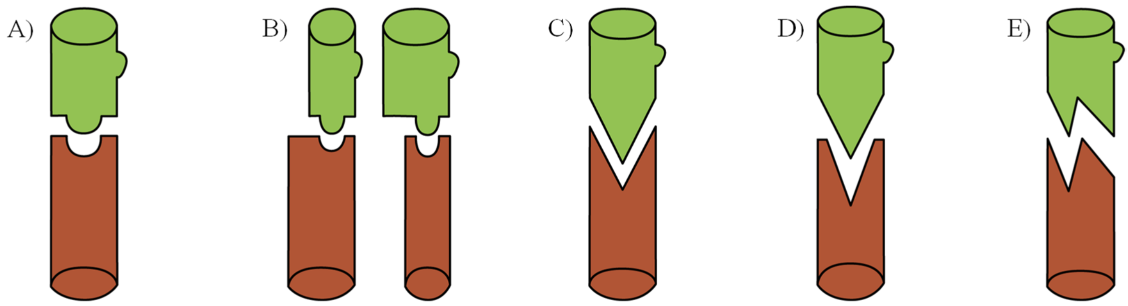

Figure 1. The different grafting methods used in this study, (**A**) Omega completely aligned (OM-CA), (**B**) Omega partially aligned (OM-PA), (**C**) V-shape (V), (**D**) Full cleft (FC) and (**E**) Whip and tongue hand-made (WTh).

The plant production protocol for all the grafting methods followed the standard commercial practices of the Vitis Navarra nursery and is detailed in Villa-Llop et al. (2025). Briefly, scions were prepared as single-bud cuttings. Rootstock raw canes were cut into 38–40 cm long cuttings and manually de-budded. All material was disinfected and stored at 4 °C with 85–90% relative humidity. Before grafting, scion and rootstock cuttings were rehydrated in tap water for 24 h. Then, an experienced worker paired scion and rootstock with similar diameter, except in the OM-PA method. After grafting, the union was dipped into melted paraffin (Stähler Rebwachs Pro®). Grafted plants were placed vertically in plastic crates filled with moist jute and sand and transferred to the stratification chambers. Callusing was carried out under controlled conditions (20–25 °C, >80% RH) for 15–20 days. When sufficient callus was visible, grafted plants were removed from the stratification chamber (Figure S1), bases were treated with rooting hormone (Chryzoplus gris®), unions re-waxed, and plants transferred to the field nursery. Grafted plants remained in the field from May to December. At the end of the growing season, they were mechanically uprooted and stored in cold chambers (4 °C) for further evaluation.

Weather data for the growing seasons was obtained from the Agroclimatic Information Service (SIAR) station located in Miranda de Arga (42°30′40.51″ N, 1°48′31.43″ W, 344 m a.s.l), obtained from the public database of the Sistema de Información Agroclimática para el Regadío (SIAR). Monthly rainfall and cumulative growing degree days (GDD) were calculated from 1 May to 31 December in each year (Figure 2). GDD was computed using daily mean air temperature, with a base threshold of 10 °C. Between May and July, rainfall and GDD patterns were similar in both years, with only minor differences. From August onwards, clear divergences were observed. In 2020, rainfall was more uniformly distributed across August, October and December, while in 2021 it was concentrated in September and November. GDD accumulation also diverged after August, with 2020 reaching slightly higher values (~1600 °C) than 2021 (~1500 °C) by the end of the season.

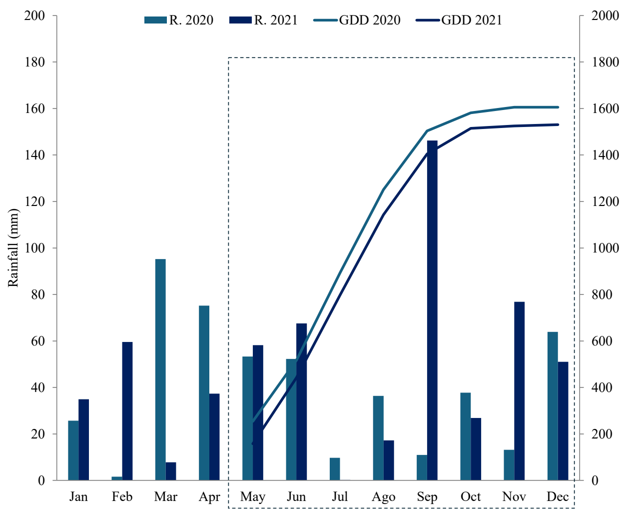

Figure 2. Monthly rainfall (bars) and cumulative growing degree days (GDD, lines) recorded in 2020 and 2021 at the experimental site.

2.2. Histological evaluation

Histological analyses were conducted after callusing and after uprooting phases, following the procedure described by Irisarri et al. (2019) with minor modifications. At each time point, five plants per grafting method were sampled. Paraffin was carefully removed from the graft union with a scalpel, avoiding damage the callus tissue. The graft union was then isolated by cutting 5 cm above and below this union using scissors. Samples were fixed in a 3:1

(v/v) solution of 95% ethanol and glacial acetic acid for 24 h and then stored in 70% ethanol at 4 °C.

Longitudinal sections of the graft union were obtained using low-profile disposable blades (Leica 819, Leica Biosystems, Wetzlar, Germany). Digital images were taken to measure, on both scion and rootstock sides, the wound length, conductive zone length, and callus extension. Wound length was defined as the total cut-surface of each partner. The conductive zone was defined as the portion of this section occupied by living tissues, excluding pith and bark. Callus extension was the length of callus tissue present at the interface. Measurements were performed using ImageJ software (v. 1.53k, National Institutes of Health, USA) and processed in Microsoft Excel® (Microsoft Corporation, USA) (Figure 3).

To evaluate the cellular development at the graft union, longitudinal sections were placed in Petri dishes and stained for 30 s with a 0.07% (w/v) solution of calcofluor (Calcofluor White stain, 18909 Sigma), a cellulose-specific dye. Stained sections were rinsed with double-distilled water to remove excess dye and then directly observed under a fluorescence microscope (Axio Imager.A2, Zeiss, Germany) equipped with a DC300 digital camera (Leica Microsystems, Germany), without the preparation of additional sections. For the analysis of callus and vascular connections, four observations were made per sample, two for each longitudinal section (Figure 4).

The cell development at the graft union was assessed using a seven-point ordinal scale, describing the progression from irregular cells to complete vascular connection (Figure 5). The categories of callus and vascular tissue development were defined as (1) irregular, unorganized cells with undefined morphology; (2) groups of few cells forming localized bundles; (3) elongated cell organization forming post-cambial tissue; (4) organized cells with visible early vessel formation; (5) differentiated conductive tissue (xylem and phloem); (6) partial vascular connection between scion and rootstock, only one side of the grafted plant was connected and (7) complete vascular connection in both sides of the graft union. Categories 3 and 4 were considered transitional stages and were observed in both callusing and uprooting phases; thus, they were pooled for analysis. For each sample, the median score from the four observations was calculated and the percentage of plants in each category was determined.

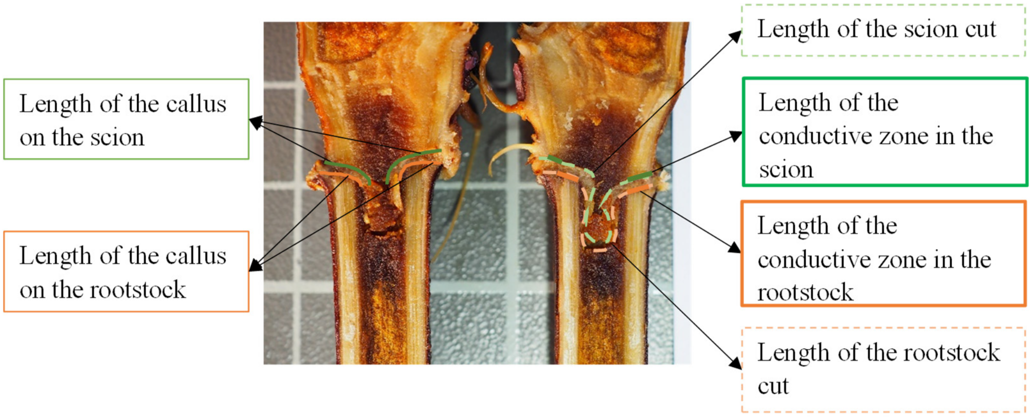

Figure 3. Visual representation of the anatomical measurements performed on longitudinal sections at the graft union. The image illustrates the method used to quantify the length of the scion and rootstock cuts (dashed line), callus length on both scion and rootstock cut surfaces (thin solid line), and the length of the conductive zone formed within the scion and rootstock (thick solid line). Green indicates measurements in the scion, while orange indicates measurements in the rootstock.

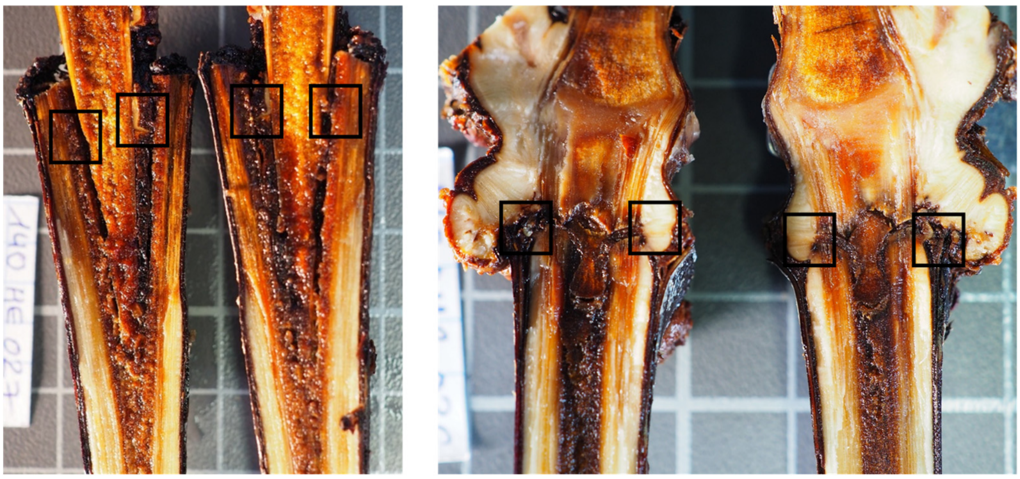

Figure 4. Longitudinal sections of cv. 'Tempranillo' grafted onto 110 Richter showing the graft union one year after grafting. Black squares indicate the four observation areas used for the histological assessment of cell development and vascular connections.

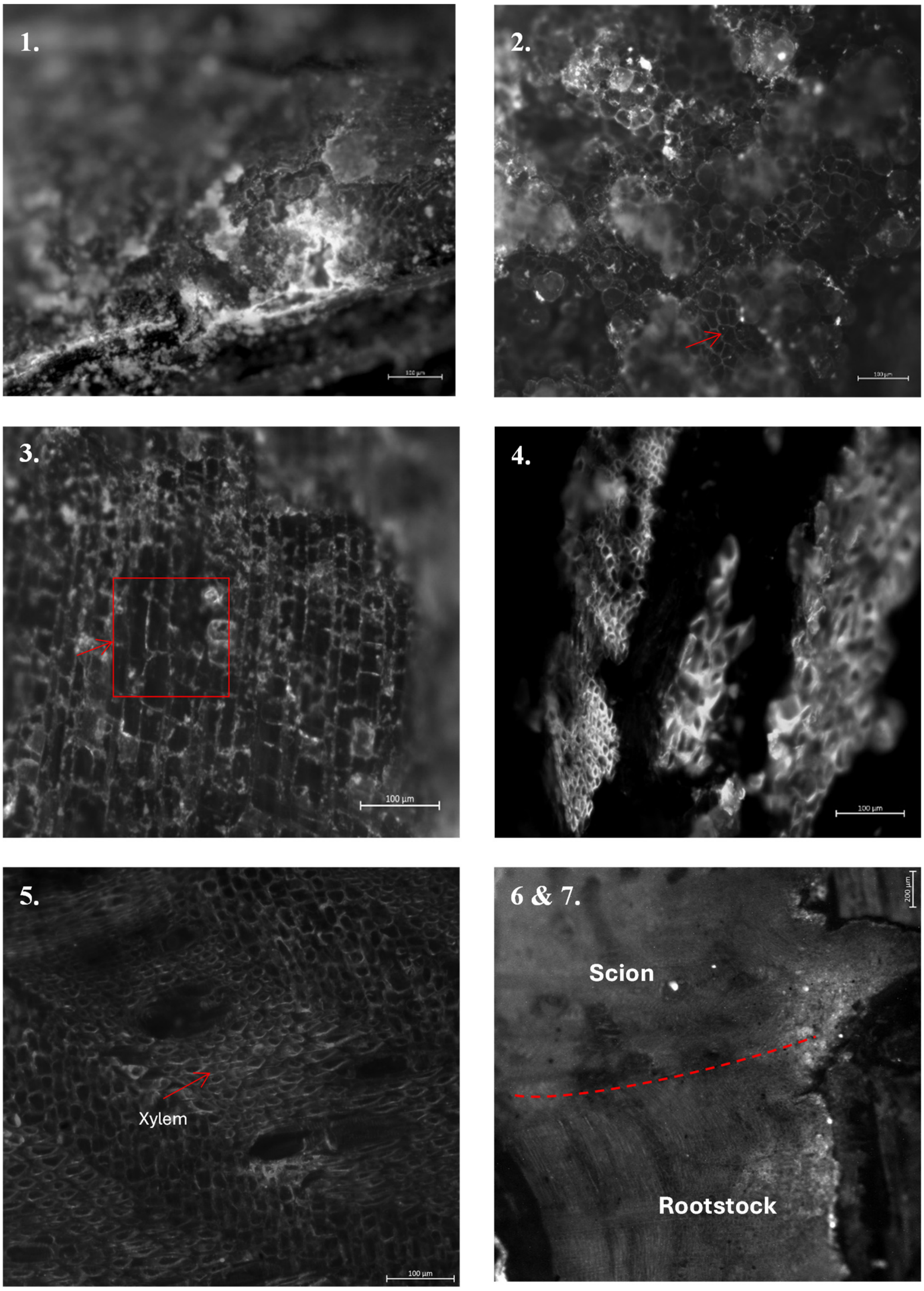

Figure 5. Fluorescence microscopy images of the seven categories used to classify cell and vascular tissue development at the graft union. Classification from unorganized callus cells (1) to fully differentiated vascular tissue with complete graft union (7). Arrows indicate 'representative structures'.

2.3. Hydraulic evaluation

The evaluation of hydraulic properties of grafted plants required establishing them for one complete season to allow new shoot development. To guarantee uniform development conditions, twenty-four grafted plants from the experimental set-up described above (Section 2.1) were planted in pots. Four of the five grafting methods considered in that experiment were included: OM-CA, OM-PA, V, and WTh, with six plants per grafting method. Plants were established at the experimental facilities of the Public University of Navarra, Pamplona, Spain (42°47′36″ N, 1°37′52″ W, 430 m a.s.l.) in April 2021. Grafted plants were grown in 20-L pots filled with a mix of vermiculite, sand, and commercial substrate. Pots were arranged in two rows in a completely randomized design, and each pot was drip irrigated twice daily for 10 min (2.3 L·h^{-1} per plant).

Following budburst in 2022, plants were trained to two shoots. Then, hydraulic conductance (K) was assessed in five uniform plants per grafting method, adapting the gravimetric method of Torres-Ruiz, Sperry, and Fernández (2012), which records water flow through the plant over time under controlled pressure gradients (Figure 6). The original protocol, developed for excised root segments, was adapted to allow measurements on whole grafted plants, which have a more complex hydraulic structure. In the pot, each plant was cut 30 cm below the graft union and 50 cm above the spur insertion point on each shoot. Immediately after cutting, the entire plant was fully submerged in a water-filled container to prevent air entry into the vascular system and was transported underwater to the laboratory.

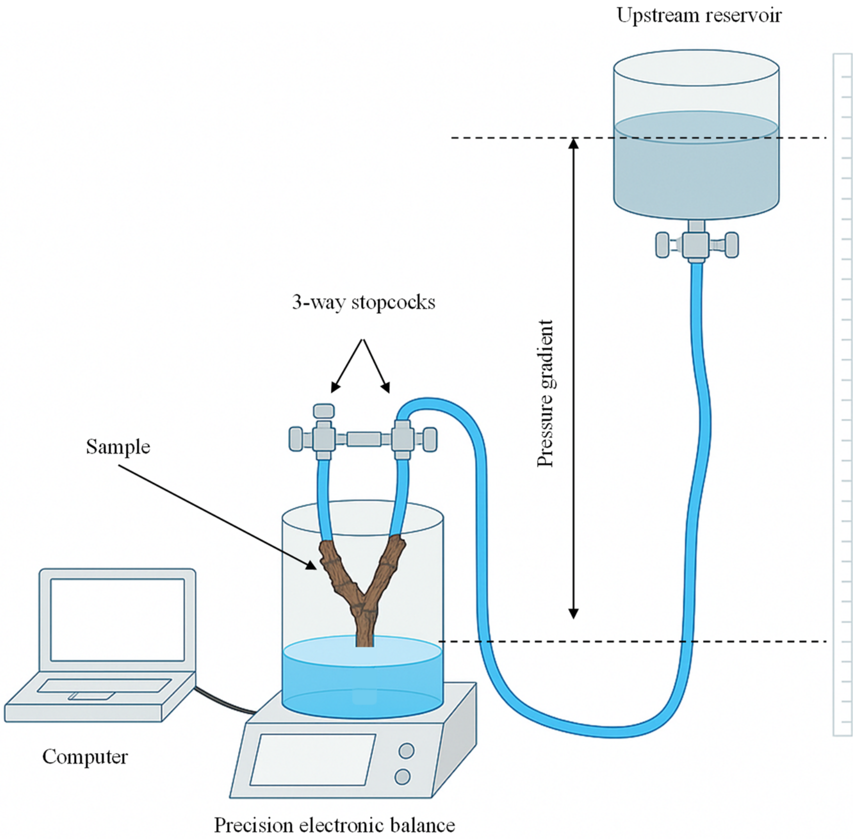

Figure 6. Experimental setup used for the gravimetric determination of hydraulic conductance in grafted plants, modified Torres-Ruiz, Sperry, & Fernández (2012). The two shoots were connected via flexible tubing to a reservoir. Pressure was adjusted by raising the height of the reservoir along a graduated vertical ruler. Water flow through the plant exited from the basal end of the rootstock and was recorded by the balance, connected to a computer for data acquisition.

All manipulations were performed under water to avoid xylem cavitation. Each shoot was recut to 5 cm above the spur insertion point, and the trunk was recut 10 cm below the graft union. The ends of the shoots were wrapped with Teflon tape and connected to silicone tubes pre-filled with degassed 20 mM KCl solution. The solution was degassed under vacuum prior to use to avoid the formation of air bubbles that could induce artificial losses in hydraulic conductivity (Venturas, Sperry, & Hacke, 2017).

The hydraulic system consisted of a closed circuit filled with the same KCl solution (Figure 6). The tubes from both shoots converged into a single tube connected to an elevated reservoir, which applied pressure to the sample. Once the system was connected, the plant was removed from the water container and suspended vertically above a Quintix 224-1S Analytical Balance (Sartorius Lab Instruments GmbH & Co., Göttingen, Germany) connected to a computer running Microsoft Excel®. The balance recorded the weight of solution exiting the basal end of the rootstock every 5 s. Water flow (F) was calculated as the change in weight over time. Pressure steps were applied in increasing order, from 10 cm to 130 cm of water column. Each pressure level was applied only once water flow had stabilized at the previous level. Once the measurement series was completed, the system was disconnected and the plant removed. Hydraulic conductance (K) was calculated as the slope of the linear regression between the water flow (F) and the applied pressure gradient (ΔP), according to the equation $K = F/\Delta P$, where F is expressed in $g \cdot s^{-1}$ and ΔP in MPa.

2.4. Vegetative development

Plant vegetative development was measured at the end of the 2021 growing season (December 2021) and shortly before sampling for hydraulic measurements (July 2022). Trunk cross-sectional area (TCSA) and shoot cross-sectional area (SCSA) were used as surrogates of vegetative development (Santesteban, Miranda, & Royo, 2010). Two perpendicular diameters were measured with a digital calliper (Mitutoyo CD67-S15PP, Kanagawa, Japan), at 10 cm below the graft union for TCSA, and at the first internode of the shoot for SCSA. At the end of winter 2021, shoot weight (SW) was also recorded with a field dynamometer (ILSA 9702, Sint-Pieters-Leeuw, Belgium).

2.5. Statistical analysis

Statistical analyses were conducted in RStudio (version 1.4.1103; RStudio Team, 2021). Data normality and homogeneity of variances were checked with Shapiro–Wilk and Levene's tests. Percentage data were arcsine square root transformed prior to the analysis. The effect of grafting method on histological, hydraulic conductance and vegetative parameters was evaluated using one-way analysis of variance (ANOVA). For all analysis, means ± standard errors (SE) were calculated. When the F-value was significant ($p \leq 0.05$), post-hoc comparisons were performed using Tukey's honest significance difference (HSD) test, implemented with the "agricolae" package (Mendiburu, 2021).

3. Results and Discussion

3.1. Histological evaluation

Grafting method influenced the geometry of cut surface at the graft union in both scion and rootstock across the two years of the experiment (Table 1 and Figure 7). Omega grafts (OM-CA and OM-PA), characterized by a horizontal cut, consistently exhibited shorter cut surface lengths than WTh, V, and FC, which were based on longitudinal cuts. This reduced surface contact was consistently associated with shorter conductive zone lengths in both graft partners. For instance, in 2021 OM-CA and OM-PA grafted plants showed the lowest cut surface lengths (23.1 and 27.2 mm in scion; 22.4 and 22.2 mm in rootstock) and conductive zone lengths (4.7 and 5.3 mm in scion; 4.9 and 6.6 mm in rootstock). By contrast, V and WTh methods nearly doubled these values (43.9 and 46.7 mm in scion; 43.7 and 46.7 mm in rootstock, for cut surface; 13 and 16.6 mm in scion; 24.1 and 18.6 mm in rootstock for conductive zone) (Table 1). These differences mainly reflected the geometry of the grafting methods: omega grafts produced a shorter and more compact interface, while V, WTh and FC resulted in longer longitudinal surfaces (Figure 7).

Grafting method influenced callus formation at the graft union, with differences across sampling times (Figure 8). In 2020, after the callusing phase, OM-PA grafts showed the highest values in both scion and rootstock tissues (close to 90%), outperforming V, WTh, and FC grafts, which remained below 60%. This trend continued after the rooting field phase, OM-PA maintained the highest values of callus along with OM-CA (≥50% in both partners), whereas WTh showed an improvement compared to the callusing phase (from <20% after callusing to >30% after rooting field). In contrast, V and FC grafts exhibited the lowest percentages of callus development in the conductive zone of the rootstock (4.9 and 19.9%, respectively). In 2021, differences among grafting methods were less pronounced after callusing, but became significant after rooting field phase. At that phase, scion callus was higher for OM-CA (above 90%), while OM-PA and V grafts remained below 80% and WTh dropped to 30%. Rootstock values followed a similar trend. Both years, callus production after the callusing phase was generally similar between scion and rootstock. However, after the rooting field phase, the production of callus in the scion conductive zone tended to exceed those observed in the rootstock, in agreement with previous reports suggesting that scion genotype often affects callusing more strongly than rootstock (Milien et al., 2012). This pattern also agrees with different studies which showed higher expression of cell-wall synthesis genes in scions than in rootstocks, suggesting that growth may be enhanced by the presence of auxin originating from the bud (Loupit et al., 2025; Melnyk et al., 2018).

Table 1. Cut surface and conductive zone lengths (mm) at the graft union for each grafting method [omega completely aligned (OM-CA), omega partially aligned (OM-PA), V-shape (V), and hand-made whip ad tongue (WTh)], measured after callusing phase (2020 and 2021).

Year	Grafting Method	Cut Surface (mm)		Conductive Zone (mm)	
		Scion	Rootstock	Scion	Rootstock
2020	OM-CA	25.1 ± 1.1 c	24.0 ± 1.1 C	4.9 ± 0.9 b	6.0 ± 0.5 B
	OM-PA	24.6 ± 0.7 c	25.9 ± 1.9 C	4.2 ± 0.9 b	5.9 ± 0.8 B
	V	42.8 ± 1.5 b	55.4 ± 6.4 B	9.4 ± 1.6 b	20.4 ± 3.6 A
	WTh	72.6 ± 6.9 a	75.4 ± 5.6 A	34.2 ± 12.0 a	25.1 ± 5.8 A
	FC	73.9 ± 3.9 a	79.3 ± 2.0 A	33.8 ± 3.7 a	14.8 ± 2.9 ab
	ANOVA	***	***	***	**
2021	OM-CA	23.1 ± 0.7 b	22.4 ± 0.8 B	4.7 ± 0.4 b	4.9 ± 0.3 B
	OM-PA	27.2 ± 1.1 b	22.2 ± 0.8 B	5.3 ± 0.5 b	6.6 ± 0.6 B
	V	43.9 ± 1.9 a	43.7 ± 1.8 A	13.0 ± 1.7 a	24.1 ± 3.2 A
	WTh	46.7 ± 5.0 a	46.7 ± 5.6 A	16.6 ± 2.8 a	18.6 ± 4.5 A
	ANOVA	***	***	***	***

Mean values ± SE (n = 5). Measurements were taken on both the scion and rootstock sides. Different lowercase and capital letters indicate significant differences ($p < 0.05$) between grafting methods within the scion and the rootstock, respectively (Tukey's test). (** $p \leq 0.01$ and *** $p \leq 0.001$).

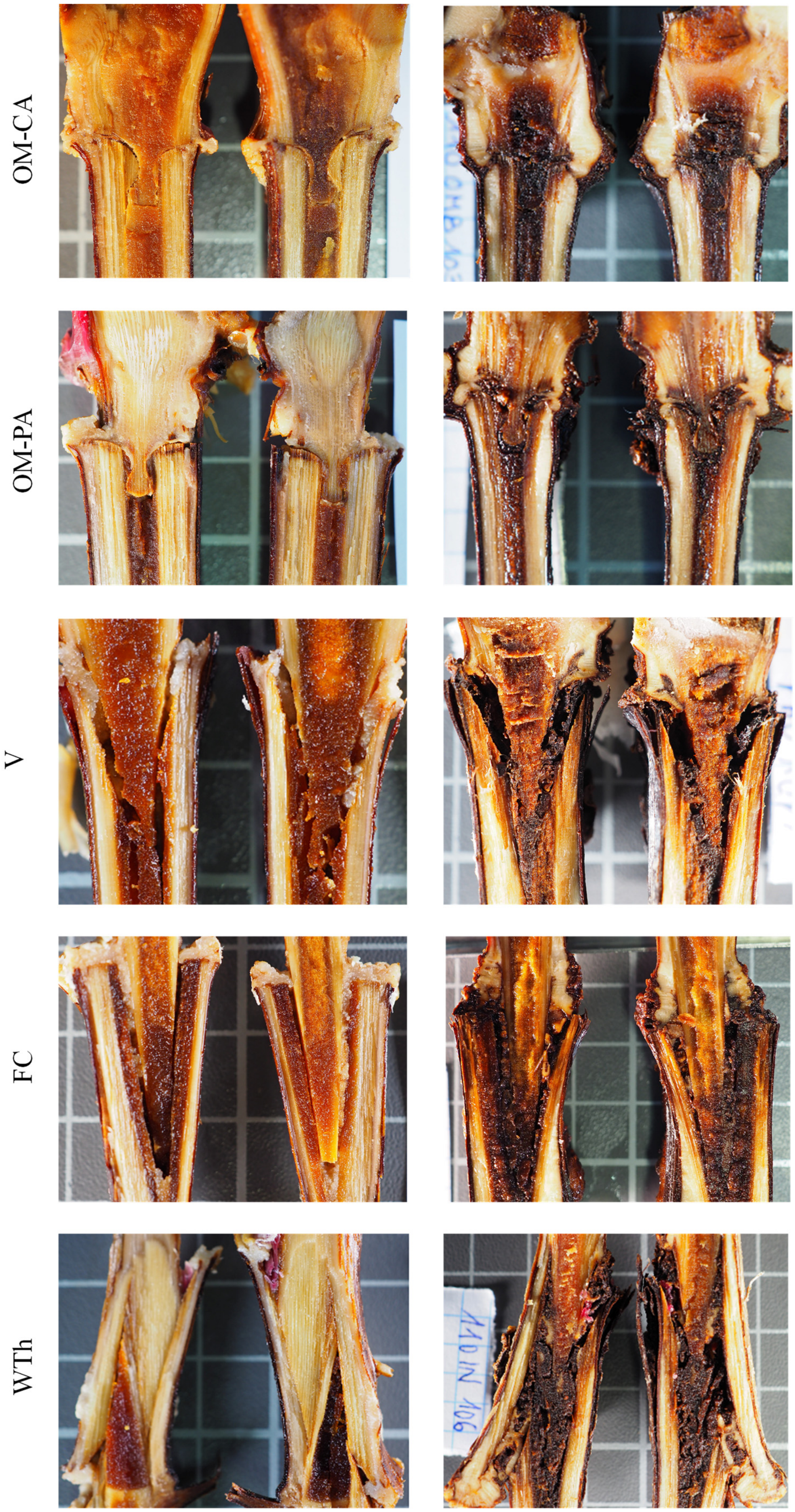

Figure 7. Longitudinal sections of the graft union after callusing (**left column**) and after rooting field (**right column**) for each grafting method showing.

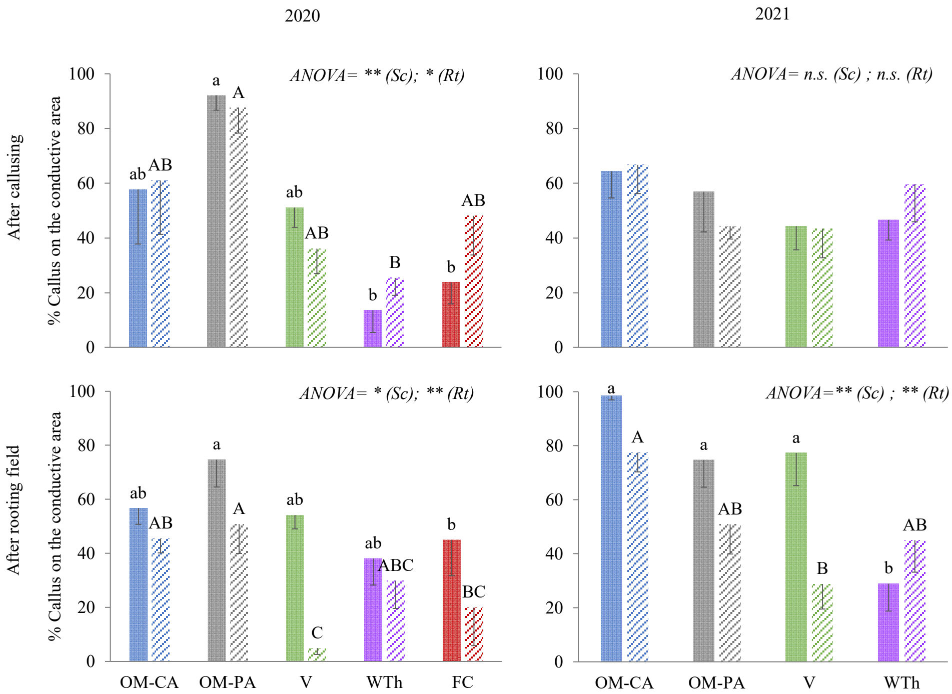

Figure 8. Percentage of callus formation on the conductive zone of the graft union in both scion and rootstock, after callusing (top row) and after rooting field (bottom row), measured in 2020 (left column) and 2021 (right column), for each grafting method OM-CA ; OM-PA ; V ; WTh ; FC . Bars represent means ± SE (n = 5). Solid bars correspond to the scion (Sc); hatched bars correspond to the rootstock (Rt). Letters indicate significant differences among grafting methods for the scion (lowercase) and rootstock (uppercase), respectively, according to Tukey's test ($p \leq 0.05$). ANOVA results for each tissue and year are shown in each panel (* $p \leq 0.05$; ** $p \leq 0.01$; n.s. = not significant).

Grafting method affected the distribution of grafted plants across cellular developmental categories (Figure 9). In 2020 after the callusing phase, most plants in all grafting methods were still in the earliest categories of callusing (categories 1–2). WTh grafts concentrated almost entirely in category 1 (80%), while OM-PA grafts were mostly in category 2 (60%). OM-CA, V and FC grafts were more uniformly distributed between categories 1 to 3, the latter already showing early vascular formations (category 4). Following the rooting field phase, distribution shifted towards more advanced categories, reflecting the progression from callus proliferation to vascular differentiation and graft union establishment (Figure 9). All grafting methods had plants in categories 4–7, OM-CA showed the highest proportion in category 7 (40%), indicative of complete vascular connection on both sides. OM-PA plants were concentrated in categories 5–6, V and WTh mainly between categories 4 and 5, and FC retained individuals in category 3 after rooting but also included plants in category 7. In 2021, a similar pattern was observed after the callusing phase with most plants still in the early stages of callusing (categories 1–2). OM-PA plants were accumulated in category 2 (80%), while OM-CA concentrated in categories 3–4, and V and WTh had higher proportions in category 1 (40% each). After the rooting field phase, OM-CA again had the highest proportion of plants in category 7 (40%), whereas OM-PA concentrated mainly in categories 5–6. V and WTh were mostly distributed between categories 4–5, without individuals reaching category 7. The limited differences between 2020 and 2021 can be explained by the similar climatic conditions during May–July (Figure 2), when grafted plants were first established in the field. This period coincides with the most sensitive stage for callus development, reducing the impact of interannual variability on early anatomical responses.

Although our classification was based on anatomical observations that may involve some observer-dependent interpretation, especially in transitional stages (categories 4 and 5), the results presented showed that cut geometry influenced callus formation and the subsequent vascular tissue development. Longer cut surfaces have often been assumed to favour vascular reconnection, but our results contradict that assumption. Callus development was generally higher in omega grafts being the shorter cut surface graft type, especially OM-PA after callusing and OM-CA after rooting field phase, while V and FC grafts showed the lowest values in the rootstock conductive zone. Categorical analysis confirmed this trend, with OM-CA plants more frequently reaching complete vascular connection, whereas WTh and V remained concentrated in intermediate stages. These findings were consistent with Battiston et al. (2022), who observed that grafting method affected the timing and extent of callus differentiation, with OM grafts showing relatively faster progression. Similarly, Camboué et al. (2025) reported through 3D micro-CT analysis that, despite shorter contact surface, OM grafts tended to present fewer air spaces and necrotic tissues at the interface compared with other grafting methods. The high variability observed in OM-PA further highlighted the importance of cambial alignment, reinforcing earlier evidence that misalignment compromises anatomical integrity (Carrere et al., 2022; Marín et al., 2022). In addition, Battiston et al. (2022) highlighted that the extent of necrosis was greater in cleft-type grafts, which coincides with our observation of lower callus coverage in V and FC methods. Likewise, Camboué et al. (2025) demonstrated that grafts passing nursery quality controls may still contained substantial proportions of non-functional tissue, underlining that external assessment alone cannot guarantee internal anatomical quality.

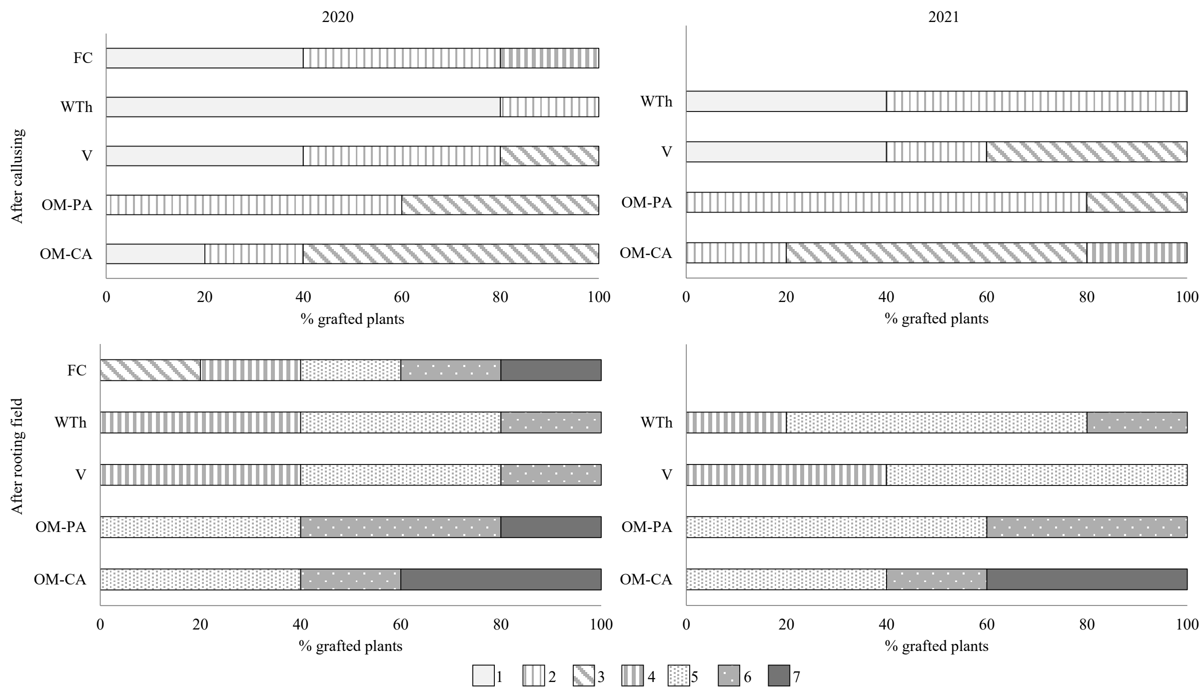

Figure 9. Distribution of grafted plants (%) across developmental categories (1 to 7), assessed after the callusing stage (top row) and after the rooting field stage (bottom row), in 2020 (left column) and 2021 (right column). (1) Irregular, unorganized cells with undefined morphology, (2) Groups of few cells forming localized bundles, (3) Elongated cell organization forming post-cambial tissue, (4) Organized cells with visible early vessel formation, (5) Differentiated conductive tissue (xylem and phloem), (6) Partial vascular connection between scion and rootstock (only one side connected), (7) Complete vascular connection in both.

3.2. Influence of graft type in plant development and hydraulic conductance

Grafting method did not influence vegetative growth in any season (Table 2). Trunk cross-sectional area (TCSA), shoot cross-sectional area (SCCA), and shoot weight (SW) were not affected by grafting at the end of the first season. However, in July 2022, grafting method affected TCSA, with WTh, OM-CA and OM-PA plants reaching the highest values and V grafts the lowest (1.96, 1.88, 1.83 and 1.42 cm^2, respectively) (Table 2).

Hydraulic conductance (K) was not significantly influenced by grafting method (Figure 10), and no significant correlations were found between K and vegetative growth parameters or anatomical classification of the graft union (data not shown). The limited number of potted plants measured per treatment (n = 5) may have reduced the statistical power to detect differences among grafting methods. In addition, the gravimetric method estimates K under controlled pressure gradients, reflecting potential conductance rather than field performance. Despite the precautions taken to prevent xylem cavitation and passive water uptake, as recommended by Torres-Ruiz, Sperry, & Fernández (2012), the occurrence of artefacts associated with cutting procedures and system stabilization cannot be completely excluded. Nevertheless, a consistent trend was observed in the distribution of values. OM-CA exhibited the highest median K, followed by V, whereas OM-PA and WTh showed lower median values (1.24, 0.93, 0.72 and 0.69 $g \cdot s^{-1} \cdot MPa^{-1}$, respectively) (Figure 10). The dispersion of data varied among grafting methods. OM-CA had a narrower interquartile range and maintained high median values, reflecting more uniform performance among replicates. In contrast, OM-PA had the widest range, from the highest to the lowest K values (2.30 and 0.26 $g \cdot s^{-1} \cdot MPa^{-1}$, respectively). V grafts showed similar but less extreme variability, while WTh combined the lowest K with smallest variability, suggesting a low K across all grafted plants. Our findings were comparable with those of Marín et al. (2020), who evaluated whole-plant and graft union hydraulic conductance in different grafting methods using the XYL'EM system. In their study, WT and V grafts showed higher conductance than OM and FC grafts, a trend partly contrasting with our observations where OM-CA exhibited the highest values. These differences may reflect methodological factors and differences in the plant material used, since Airen was used as scion and measurements were performed on one-year old grafted plants just after the uprooting phase. Nevertheless, other studies confirmed that the graft union constituted the main hydraulic limitation in the grafted plant (De Herralde et al., 2006), and that differences among grafting methods could be detected at this stage. Importantly, our results highlighted that cambial alignment (OM-CA vs OM-PA) strongly modulated K, complementing previous evidence that the quality of vascular reconnection rather than the absolute contact area determined functional performance (Villa-Llop et al., 2025).

Table 2. Shoot weight (SW), trunk cross-sectional area (TCSA), and shoot cross-sectional area (SCCA) of potted grafted-plants obtained by different grafting methods [omega completely aligned (OM-CA), omega partially aligned (OM-PA), V-shape (V), and hand-made whip ad tongue (WTh)]. Measurements were taken in December 2021 and July 2022.

Grafting Method	2021			2022	
	SW (g)	TCSA (cm^2)	SCSA (mm^2)	TCSA (cm^2)	SCSA (mm^2)
OM-CA	105.5 ± 7.2	1.74 ± 0.17	47.6 ± 3.3	1.88 ± 0.04 a	115.5 ± 12.9
OM-PA	105.2 ± 16.2	1.71 ± 0.15	64.7 ± 8.2	1.83 ± 0.11 a	108.7 ± 11.9
V	91.8 ± 15.9	1.31 ± 0.09	57.9 ± 5.1	1.42 ± 0.05 b	112.7 ± 5.6
WTh	109.1 ± 5.8	1.73 ± 0.24	46.9 ± 3.7	1.96 ± 0.09 a	104.1 ± 8.1
ANOVA	*n.s.*	*n.s.*	*n.s.*	**	*n.s.*

Mean values ± SE (n = 5). Different letters indicate significant differences according to Tukey's test ($p < 0.05$). (** $p \leq 0.01$ and n.s.: non-significant).

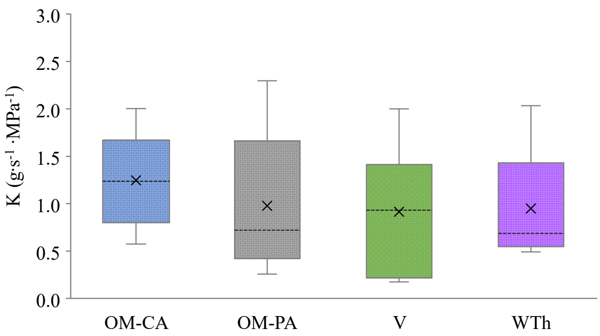

Figure 10. Boxplot of the hydraulic conductance (K) values measured over the four different grafting methods: omega completely aligned (OM-CA), omega partially aligned (OM-PA), V-shape (V), and hand-made whip ad tongue (WTh).

The absence of significant differences in hydraulic conductance among grafting methods suggested that early functional performance may converge across methods, even when anatomical contrasts were evident. This aligned with Battiston et al. (2022), who observed that differences in callus development did not always translate into clear hydraulic disparities. Camboué et al. (2025) also reported that non-functional tissue at the graft union did not necessarily compromise water transport in the short term. However, the wide range of values recorded in OM-PA plants may be relevant for vineyard establishment, as plant-to-plant variability could translate into uneven vigour in the field, a concern already highlighted by growers and nursery professionals (Marín et al., 2022; Waite, Whitelaw-Weckert, & Torley, 2015). Structural differences at the graft union may affect not only water transport but also the transmission of chemical signals involved in stomatal regulation and stress responses (Soar, Dry, & Loveys, 2006). In the present study, such physiological processes were not assessed, and no clear differences in hydraulic performance were detected among grafting methods under the experimental conditions evaluated. However, integrating these physiological parameters would allow a more precise interpretation of the effects of graft alignment and grafting method. Overall, anatomical and hydraulic traits at the graft union are influenced not only by grafting method and cambial alignment, but also by the scion–rootstock combination. Previous studies in grapevine have shown that scion–rootstock interactions can modify vegetative growth and vascular system structure, including xylem vessel characteristics, with responses varying among genotype combinations (Santarosa et al., 2016; Tandonnet et al., 2010). In addition, Milien et al. (2012) demonstrated that different genotypes within the same cultivar grafted onto a common rootstock (Syrah on 110R) exhibited contrasting callus proliferation and vascular reconnection, highlighting the influence of scion-rootstock interactions on graft union development. In the present study, only one scion–rootstock combination (Tempranillo VN69/110R) was evaluated. Consequently, differences in the parameters assessed may happen for other scion–rootstock combinations.

3.3. Implications

Omega grafts (OM-CA and OM-PA), despite having shorter cut surfaces and conductive zones, generally showed higher callus formation and a greater proportion of grafted plants achieving complete vascular connection. Under the current nursery production conditions, characterised by short callusing periods and high temperature and humidity, methods such as V, WTh, and FC appeared less favourable for vascular cambium development. These methods produced longer cambium contact surfaces but tended to have lower callus coverage and a large proportion of this callus underwent necrosis without differentiating into conductive tissue, resulting in slower vascular differentiation.

Differences in hydraulic conductance among methods were not significant, although OM-CA showed the highest and most uniform values.

While advanced three-dimensional imaging has provided detailed descriptions of the graft interface (Camboué et al., 2025; Janoueix et al., 2024), its application was limited to small sample sizes and specialized infrastructures. The present study showed that simpler approaches could also provide reproducible information on graft development at scales compatible with nursery trials. These methodologies therefore represented a valuable complement to imaging, enabling the evaluation of larger plant populations and providing a practical framework for comparing grafting methods under commercial conditions. Future research could benefit from integrating these scalable techniques with advanced imaging, enabling the connection of large datasets to high-resolution anatomical. Such integration would allow a more accurate quantification of the continuity and distribution of functional vessels at the graft union, and a better understanding of the relationship between anatomical features (e.g., air spaces or necrotic tissues) and vascular functionality.

Taken together, our results confirmed that OM grafts, often criticised by practitioners, could achieve equal or superior anatomical and functional outcomes compared with alternative methods, at least during the nursery stage evaluated in this study. This was consistent with recent findings from Villa-Llop et al. (2025), who reported no evidence that OM grafts compromised vineyard performance during the first productive years. However, the present work focused on early developmental stages, and long-term vineyard performance was not assessed. The persistence of structural irregularities in some methods and the variability associated with partial alignment therefore highlighted the need for extended field monitoring. Further studies combining scalable evaluations such as those applied here with advanced imaging approaches could clarify whether early anatomical traits at the graft union are predictive of vineyard longevity.

Supplementary Materials

The additional data and information can be downloaded at: https://media.sciltp.com/articles/others/2603130835558120/PlantEcophys-25100091-Supplementary-Material.pdf.

Author Contributions

AV-L: formal analysis, investigation, methodology, resources, writing—original draft preparation, software; SC-M: investigation, writing—reviewing and editing; ML: investigation; AP: supervision; PI: supervision, writing—reviewing and editing; LGS: funding acquisition, project administration, writing—reviewing and editing. All authors have read and agreed to the published version of the manuscript.

Funding

This work was supported by the projects EFA 324/19—VITES QUALITAS and EFA 033/01—VITRES, 65% co-funded by the European Regional Development Fund (ERDF) through the Interreg Programs V-A Spain-France-Andorra (POCTEFA 2014–2020) and VI-A Spain-France-Andorra (POCTEFA 2021–2027), aimed at enhancing cross-border economic and social integration.

Data Availability Statement

Data are available from AV-L on request.

Acknowledgments

The authors thank technical team at Vitis Navarra nursery, especially Rafael García and Javier Eraso, for their collaboration.

Conflicts of Interest

The authors declare no conflict of interest.

Use of AI and AI-Assisted Technologies

During the preparation of this work, the authors used ChatGPT to generate the icons included in Figure 6. After using this tool, the authors reviewed and edited the content as needed and take full responsibility for the content of the published article.

Peer Review Statement

Plant Ecophysiology acknowledges the contributions of two anonymous reviewers to the peer review of this manuscript.

References

Bahar E, Korkutal I, Carbonneau A, & Akcay G. (2010). Using magnetic resonance imaging technique (MRI) to investigate graft connection and its relation to reddening discoloration in grape leaves. *Journal of Food, Agriculture and Environment*, *8*, 293–297.

Battiston E, Falsini S, Giovannelli A, Schiff S, Tani C, Panaiia R, Papini A, Di Marco S, & Mugnai L. (2022). Xylem anatomy and hydraulic traits in *Vitis* grafted cuttings in view of their impact on the young grapevine decline. *Frontiers in Plant Science*, *13*. https://doi.org/10.3389/fpls.2022.1006835.

Camboué M, Janoueix A, Spilmont A-S, Mathieu G, Ollat N, Santesteban LG, & Cookson S. (2025). Visualising xylem vessels connections formed one year after grafting using different techniques. *OENO One*, *59*(3), 3. https://doi.org/10.20870/oeno-one.2025.59.3.9148.

Carrere C, Spilmont A-S, Loupit G, Beutin P, Stessels C, Ollat N, & Cookson S-J. (2022). Evaluation of criteria to assist the selection of good quality grafted grapevines prior to their commercialisation. *OENO One*, *56*(2), 2. https://doi.org/10.20870/oeno-one.2022.56.2.4792.

De Herralde, F, del Mar Alsina M, Aranda X, Savé R, & Biel C. (2006). Effects of rootstock and irrigation regime on hydraulic architecture of *Vitis vinifera* L. cv. Tempranillo. *OENO One*, *40*(3), 3. https://doi.org/10.20870/oeno-one.2006.40.3.868.

Irisarri P, Zhebentyayeva T, Errea P, & Pina A. (2019). Inheritance of self- and graft-incompatibility traits in an F 1 apricot progeny. *PLoS ONE*, *14*(5), 1–14. https://doi.org/10.1371/journal.pone.0216371.

Janoueix A, Spilmont A-S, Moisy C, Mathieu G, Cordelières F, Teillon J, Gonzaga Santesteban L, Villa-Llop A, Crespo S, Marín D, & Cookson SJ. (2024). Imaging xylem connections between the scion and rootstock of grafted grapevine with X-ray microtomography. *Acta Horticulturae*, *1390*, 103–108. https://doi.org/10.17660/ActaHortic.2024.1390.13.

Korkutal İ, Bahar E, & Ozdemir AG. (2018). Determining the internal connection ratios by MRI and their effects on grafted rooted vine growing features of cvs. Merlot and Syrah. *Erwerbs-Obstbau*, *60*(1), 61–69. https://doi.org/10.1007/s10341-018-0404-8.

Loupit G, Valls Fonayet J, Tran J, Garcia V, Hummel I, Petriacq P, Gallusci P, Berger M, Franc C, de Revel G, Ollat N, & Cookson SJ. (2025). Graft union formation involves interactions among bud signals, carbon availability, dormancy release, wound responses and non-self-communication in grapevine. *The Plant Journal*, *122*(5), e70244. https://doi.org/10.1111/tpj.70244.

Marín D, Mayor B, Santesteban LG, Miranda C, Urrestarazu J, Abad FJ, Savé R, Aranda X, de Herralde F. (2019). The grapevine nursery sector in Spain/ A szőlőiskola-szektor Spanyolországban. In *Phytoremediation of Soil Contaminated with Cadmium* (pp. 109–119). Doktoranduszok Országos Szövetsége, Akadémiai Kiadó.

Marín D, Abad FJ, Torres-Ruiz JM, & Santesteban LG. (2020). *The vascular connections in grafted plants under examination*. XIIIth International Terroir Congress. https://www.researchgate.net/publication/346336075_The_vascular_connections_in_grafted_plants_under_examination.

Marín D, Santesteban LG, Dayer S, Villa-Llop A, Abad FJ, Gambetta GA, Torres-Ruiz JM, & Torres N. (2022). Connection matters: Exploring the implications of scion–rootstock alignment in grafted grapevines. *Australian Journal of Grape and Wine Research*, *28*(4), 561–571. https://doi.org/10.1111/ajgw.12559.

Mary S, Laveau C, Lecomte P, Birebent M, & Roby J-P. (2017). Impact of grafting type on Esca foliar symptoms. *OENO One*, *51*(2), 221–230. https://doi.org/10.20870/oeno-one.2016.50.4.1408.

Melnyk CW. (2017). Plant grafting: Insights into tissue regeneration. *Regeneration*, *4*(1), 3–14. https://doi.org/10.1002/reg2.71.

Melnyk CW, Gabel A, Hardcastle TJ, Robinson S, Miyashima S, Grosse I, & Meyerowitz EM. (2018). Transcriptome dynamics at Arabidopsis graft junctions reveal an intertissue recognition mechanism that activates vascular regeneration. *Proceedings of the National Academy of Sciences*, 115(10), E2447–E2456. https://doi.org/10.1073/pnas.1718263115.

Melnyk CW, & Meyerowitz EM. (2015). Plant grafting. *Current Biology*, *25*(5), R183–R188. https://doi.org/10.1016/j.cub.2015.01.029.

Mendiburu F. (2021). *Agricolae: Statistical Procedures for Agricultural Research* (Version 1.3-5) [Computer software]. https://CRAN.R-project.org/package=agricolae.

Milien M, Renault-Spilmont A-S, Cookson SJ, Sarrazin A, & Verdeil J-L. (2012). Visualization of the 3D structure of the graft union of grapevine using X-ray tomography. *Scientia Horticulturae*, *144*, 130–140. https://doi.org/10.1016/j.scienta.2012.06.045.

Mudge K, Janick J, Scofield S, & Goldschmidt EE. (2009). A History of grafting. In Janick J., (Ed.) *Horticultural Reviews* (1st ed., pp. 437–493). Wiley. https://doi.org/10.1002/9780470593776.ch9.

Ollat N, Bordenave L, Tandonnet JP, Boursiquot JM, & Marguerit E. (2016). Grapevine rootstocks: Origins and perspectives. *Acta Horticulturae*, *1136*, 11–22. https://doi.org/10.17660/ActaHortic.2016.1136.2.

Pina A, Cookson SJ, Calatayud A, Trinchera A, & Errea P. (2017). Physiological and molecular mechanisms underlying graft compatibility. *Vegetable Grafting: Principles and Practices*, 132–154. https://doi.org/10.1079/9781780648972.0132.

Pina A, & Errea P. (2005). A review of new advances in mechanism of graft compatibility–incompatibility. *Scientia Horticulturae*, *106*(1), 1–11. https://doi.org/10.1016/j.scienta.2005.04.003.

RStudio Team. (2021). *RStudio: Integrated development for R* [Computer software]. RStudio. http://www.rstudio.com/.

Santarosa E, Souza PVD, de Araujo Mariath JE, & Lourosa GV. (2016). Physiological interaction between rootstock-scion: Effects on xylem vessels in Cabernet Sauvignon and Merlot grapevines. *American Journal of Enology and Viticulture*, *67*(1), 65–76. https://doi.org/10.5344/ajev.2015.15003.

Santesteban LG, Miranda C, & Royo JB. (2010). Vegetative growth, reproductive development and vineyard balance. In *Methodologies and Results in Grapevine Research* (pp. 45–56). Springer. https://doi.org/10.1007/978-90-481-9283-0_4.

Soar CJ, Dry PR, & Loveys BR. (2006). Scion photosynthesis and leaf gas exchange in *Vitis vinifera* L. cv. Shiraz: Mediation of rootstock effects via xylem sap ABA. *Australian Journal of Grape and Wine Research*, 12(2), 82–96. https://doi.org/10.1111/j.1755-0238.2006.tb00047.x.

Spilmont A-S, Carrere C, Hmedi Y, & Mathieu G. (2021). X-Ray tomography: A promising tool to assess the selection of good quality grafted vines prior to their commercialization. *Internet Journal of Viticulture and Enology, 8.*

Stamp JA. (2001). The contribution of imperfections in nursery stock to the decline of young vines in California. *Phytopathologia Mediterranea*, *40*, 369–375. https://doi.org/10.14601/Phytopathol_Mediterr-1640.

Tandonnet JP, Cookson SJ, Vivin P, & Ollat N. (2010). Scion genotype controls biomass allocation and root development in grafted grapevine. *Australian Journal of Grape and Wine Research*, *16*(2), 290-300. https://doi.org/10.1111/j.1755-0238.2009.00090.x.

Tedesco S, Irisarri P, Teixeira Santos M, Fevereiro P, Pina A, & Kragler F. (2023). Early detection of grapevine graft incompatibility: Insights into translocated and virus-induced incompatibility. *Scientia Horticulturae*, *318*, 112087. https://doi.org/10.1016/j.scienta.2023.112087.

Torres-Ruiz JM, Sperry JS, & Fernández JE. (2012). Improving xylem hydraulic conductivity measurements by correcting the error caused by passive water uptake. *Physiologia Plantarum*, *146*(2), 129–135. https://doi.org/10.1111/j.1399-3054.2012.01619.x.

Venturas MD, Sperry JS, & Hacke UG. (2017). Plant xylem hydraulics: What we understand, current research, and future challenges. *Journal of Integrative Plant Biology*, *59*(6), 356–389. https://doi.org/10.1111/jipb.12534.

Villa-Llop A, Torres N, Loidi M, Velaz M, Galar-Martínez M, Crespo-Martínez S, & Santesteban LG. (2025). Does omega-type graft compromise vine performance? Evaluation of five bench grafting methods across nursery, vineyard establishment, and first productive years. *Scientia Horticulturae*, *350*, 114346. https://doi.org/10.1016/j.scienta.2025.114346.

Waite H, Whitelaw-Weckert M, & Torley P. (2015). Grapevine propagation: Principles and methods for the production of high-quality grapevine planting material. *New Zealand Journal of Crop and Horticultural Science*, *43*(2), 144–161. https://doi.org/10.1080/01140671.2014.978340.